主办 中国科学院遥感与数字地球研究所
中国地理学会环境遥感分会
出版 科学出版社

JOURNAL OF REMOTE SENSING

遥感学报

2013年 Vol.17 第17卷 No.4 第4期 ISSN 1007-4619 CN11-3841 / TP CODEN YXAUAB

2010年中国土地覆被遥感监测数据集（ChinaCover2010）

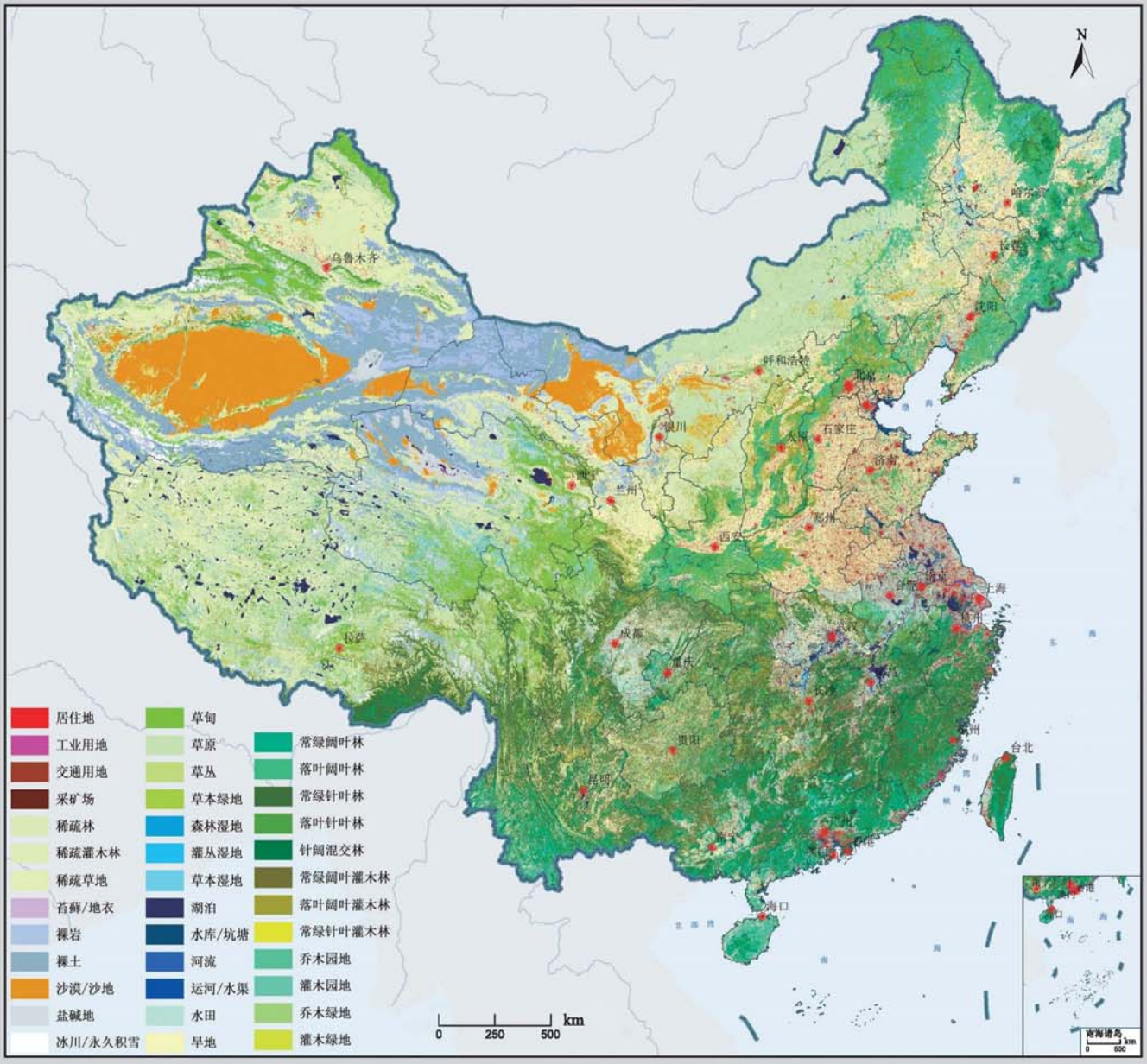

百种中国杰出学术期刊

遥感学报

Yaogan Xuebao

第 17 卷　　第 4 期　　2013 年 7 月

目　　次

JOURNAL OF REMOTE SENSING

(Vol. 17 No. 4 July, 2013)

CONTENTS

(to be continued to Inside Back Cover)

(continued from Contents page)

Haze: Remote Sensing

Remote sensing estimation of aerosol composition and radiative effects in haze days

WEI Peng[1,2], LI Zhengqiang[1], WANG Yan[1], XIE Yisong[1,2], ZHANG Ying[1,2], XU Hua[1]

1. *State Environmental Protection Key Laboratory of Satellites Remote Sensing, Institute of Remote Sensing and Digital Earth of Chinese Academy of Sciences, Beijing* 100101, *China*;
2. *University of Chinese Academy of Sciences, Beijing* 100049, *China*

Abstract: We analyzed aerosol optical, physical properties in Beijing city in January of 2013 based on ground-based remote sensing data, and used radiative transfer model to estimate aerosol radiative forcing. The results show that water-soluble Aerosol Optical Depth (AOD) increases rapidly in haze days, and contributes most to the total AOD(>70%), black carbon aerosol AOD increasesalso in haze days, which is about eight times larger than clear days. The direct radiative forcing caused by aerosol is significant, but different aerosol compositions have different effects.Black carbon dominatesforcing in the atmosphere (>57%), while water-soluble dominates in surface forcing(>60%).

Key words: anthropogenic aerosol, haze, radiative effects, ground-based remote sensing

CLC number: X87 **Document code**: A

Citation format: **Wei P, Li Z Q, Wang Y, Xie Y S, Zhang Y and Xu Hua. 2013. Remote sensing estimation of aerosol composition and radiative effects in haze days. Journal of Remote Sensing, 17(4): 1021-1031 [DOI: 10.11834/jrs.20133080]**

1 INTRODUCTION

Atmospheric aerosol plays an important role in earth's energy budget andpresents in direct forcing by scattering and absorbing radiation, and indirect forcing which by changing microphysicalproperties and radiation characteristics of clouds (Ramanathan, et al.,2001; Kaufman, et al., 2005). According to the variation of aerosol sources, we can divides aerosol into natural and anthropogenic types. Natural aerosol mainly contains volcanic ash, sea salt, dust aerosol and so on. Anthropogenic aerosol mainly containsblack carbon aerosol which is generated by mineral combustion, sulfates and nitrates aerosol which are generated by industrial emission and automobile exhaust. Different aerosoltypes have distinguished scattering and absorbing properties, also they have different radiative forcing, such as negative effect of sulfate aerosol because of strong scattering properties, andis positive ofsoot aerosol because of strong absorbing(Penner, et al., 1998). Many works focused on radiation characteristics and climatic effects of aerosol(Pilinis, et al., 1995; Satheesh, et al., 2000). However, there still exists great uncertainties in estimating radiative forcing of anthropogenic aerosol. To estimate anthropogenic aerosol radiation, model simulation (Haywood, et al., 1997; Yu, et al., 2004; Heald, et al., 2006), satellite remote sensing (Kaufman, et al., 2005), regional climate model (Wang, et al., 2002; Liu, et al., 2012) and chemical transfer mode(Zhang, et al., 2001) were used. In this paper, ground-based remote sensing measurements and aerosol model were used to analysis the aerosol components in haze days of Beijing region (January of 2013), as well asestimation of aerosol direct forcing by radiation transfer model.

2 DATA AND METHOD

2.1 Data

Our instruments located on the roof of the Institute of Remote Sensing and Digital Earth, Chinese Academy of Sciences building, containCE-318 sun-sky radiometer and AE-51 hand-held aethalometer.The data used in this paper contain: (1) Aerosol Optical Depth (AOD) (440 nm, 500 nm, 675 nm, 870 nm, 1020 nm), Single Scattering Albedo (SSA) and asymmetry parameter g (440 nm, 675 nm, 870 nm, 1020 nm), and water vapor column concentrationobtained from AOD; (2) black carbon mass concentration measured by AE-51 hand-held aethalometer (Hansen, et al., 1984); (3) relative humidity RH% obtained from China Meteorological Administration.A summary of instruments and data information are given in Table 1.

Table 1 Instruments and data

Instruments	Measurements	Period	Measurement days/d
CE-318	AOD、SSA、g water vapor column concentration	2013-01-01—2013-01-28	17
AE-51	Black carbon mass concentration	2013-01-01—2013-01-28	12
CMA	Relative Humidity (RH)	2013-01-01—2013-01-28	28

Received: 2013-04-07; **Accepted**: 2013-05-31; **Version of record first published**: 2013-06-07

Foundation: National Major Scientific Research Program (No.2010CB950800); Strategic Priority Research Program of the Chinese Academy of Sciences (No. KZZD-EW-TZ-09)

First author biography: Wei Peng (1989—), male, master candidate. He majors in atmospheric remote sensing. E-mail:wp5621679@163.com

Corresponding author biography: LI Zhengqiang (1977—), male, professor, his research interest is environment remote sensing. E-mail: lizq@irsa.ac.cn

2.2 Aerosol model

In order to estimates aerosol component optical properties, Optical Properties of Aerosol and Clouds (OPAC) model were used in this paper. OPAC model was developed by Hess (1998) for calculating aerosol andcloudoptical and microphysical properties in variegated condition. OPAC model contains water-soluble (which mainly consist of sulfates, nitrates), dust, black carbon, insoluble (which mainly contain insoluble organic matter) and sea salt aerosols. Multiwavelength (0.35—4.0 μm) optical and microphysical properties can be calculated by OPAC, like AOD, extinction and scattering coefficients, SSA and g. According to previous studies (Wang, et al., 2012; Shi, et al., 2012, Wang, et al., 2013), we selected four aerosol types as Beijing aerosol component: Black Carbon (BC), Water-Soluble (WASO), Dust (DUST), and Insoluble (INSO).

Aerosol mixing can be divided into two types: external mixed and internal mixed. In OPAC model, external mixingis used, which means the total optical properties is the sum of individuals (Hess, et al., 1998). AOD, SSA and g are calculated as below,

$$\mathrm{AOD}_\lambda = \sum_i \int \pi r^2 b_{i,\lambda}^{\mathrm{ext}} n_i(r)\,\mathrm{d}r \tag{1}$$

$$\mathrm{SSA}_\lambda = \frac{\sum_i b_{i,\lambda}^{\mathrm{ext}} \mathrm{SSA}_{i,\lambda}}{\sum_i b_{i,\lambda}^{\mathrm{ext}}} \tag{2}$$

$$g_\lambda = \frac{\sum_i b_{i,\lambda}^{\mathrm{sca}} g_{i,\lambda}}{\sum_i b_{i,\lambda}^{\mathrm{sca}}} \tag{3}$$

where λ is thewavelength, i represents different aerosol type, r is aerosol radius, $n_i(r)$ is number size distribution, $b_{i,\lambda}^{\mathrm{ext}}$, $b_{i,\lambda}^{\mathrm{sca}}$ are the extinction and scattering coefficients of the individual aerosol at a given wavelength, $g_{i,\lambda}$ is the asymmetry parameter of the individual component at a given wavelength. In OPAC model, there exists a lineal relationship between extinction coefficients of individual aerosol and number concentration and thus we can obtain aerosol extinction coefficients by changing number concentration. We set AOD, SSA, g and RH% as input, and change different aerosol number concentration until following conditions satisfied: (1) The differences of AOD measurements and simulationsare less than 0.05, (2) The differences between simulation (SSA, g) and retrieval (SSA, g) should be less than 0.05. The final results are components number concentration. Another factor to be considered is the spectral match of the optical properties, because the wavelengths in the model are 450 nm, 500 nm, 650 nm, 900 nm, 1000 nm, so the measurements should also be interpolated into the model wavelength. The flow chart is shown in Fig.1.

We selected clean day (January 2, AQI=39) and heavy haze day (January 11, AQI=386) as representations. In Fig.2, solid line represents measurements and dotted line represents AOD fitting values.The fitting values are found to be limited within the standard deviations of the measurements.

2.3 Radiative transfer model

Santa Barbara DISORT Atmospheric Radiative Transfer (SBDART) model was developed by Ricchiazzi (1998) which was used for performing the radiative transfer calculation in the shortwave (0.25—4.0 μm) region, and calculating aerosol radiative forcing (Babu, et al., 2002; Tripathi, et al., 2005). The deviations between fluxs measurements and model calculations are general within2% (Michalsky, et al., 2006).The SBDART model uses six standard atmospheres to model the standard vertical profiles: tropical, mid-latitude summer, mid-latitude winter, subarctic summer, subarctic winter, and US62. In this paper, mid-latitude winter was selected. The surface albedo of 0.15

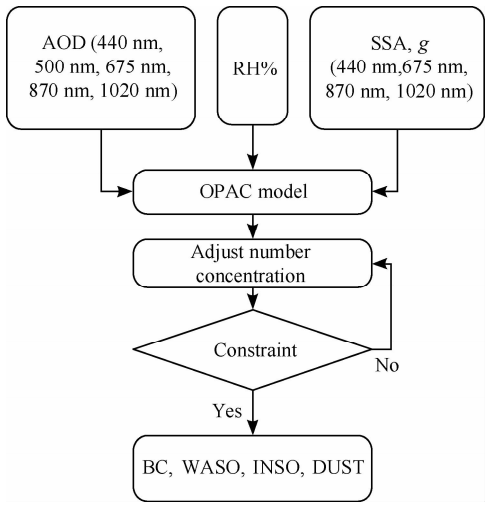

Fig.1 Flow chart of aerosol compoent retrieval

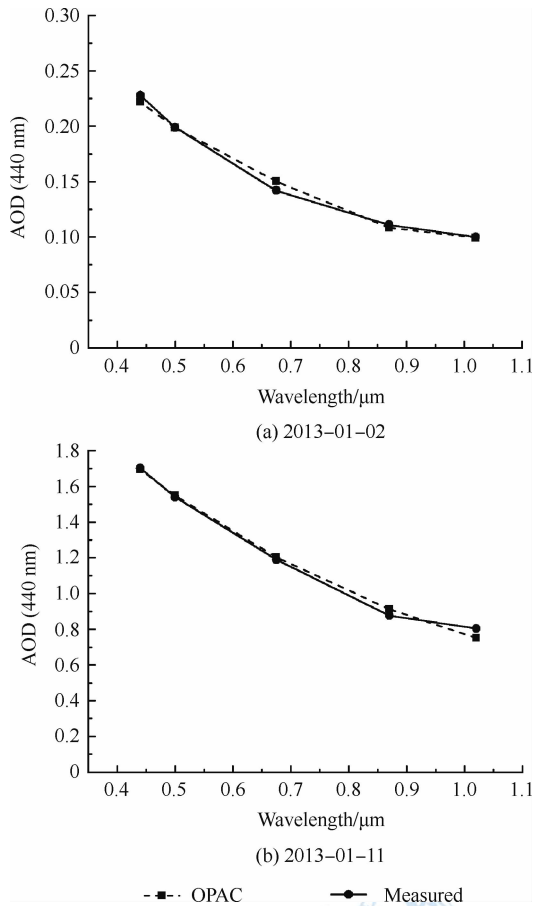

Fig.2 Results of fitting OPAC model

(Jiang, 2007) was employed. SBDART allows us to define aerosol type which contains AOD, SSA and g.Aerosol radiative forcing at the top of the atmosphere and surface are calculated as the change between the flux with and without aerosols,

$$DRF_{TOA} = FLUX(TOA)_{aerosol} - FLUX(TOA)_{no} \quad (4)$$

$$DRF_{SUF} = FLUX(SUF)_{aerosol} - FLUX(SUF)_{no} \quad (5)$$

where DRF_{TOA} is aerosol radiative forcing at the top of the atmosphere, DRF_{SUF} is surface aerosol radiative forcing, $FLUX_{aerosol}$ is radiant flux at the top of the atmosphere with aerosol condition, while $FLUX_{no}$ is clean sky condition.

Atmosphere forcing(ATM) is obtained:

$$DRF_{ATM} = DRF_{TOA} - DRF_{SUF} \quad (6)$$

According to Eq.(4)—Eq.(6), the aerosol direct radiative forcing can be obtained.

3 RESULTS AND ANALYSIS

According to the aerosol model introduced in section 2, different aerosol components were computed and compared with measurements, then direct radiative forcing was estimated.

3.1 Black carbon mass concentration estimation and validation

We compared daily average values of measurements with retrievals, the validdate is 12 days. According to the relationship between number concentration and mass concentration, black carbon mass concentration was obtained and compared with daily measurement values, as shown in Fig.3, we found R^2 = 0.66 and relative error of 32%.

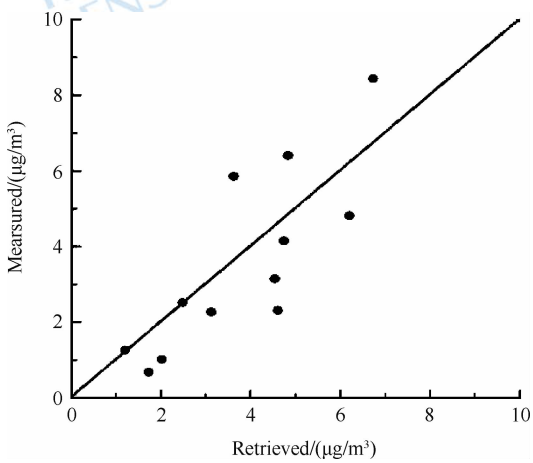

Fig.3 Comparison between measured and retrieved black carbon

3.2 Aerosol components and optical properties

Aerosol component mass fractions and AOD monthly average proportion in Beijing region were computed, as shown in Fig.4.

According to Fig.4(a), DUST (49.8%) and WASO (35.3%) mass proportion are dominated in Beijing. Ground-based sampling measurements showed the same results (Duan, et al., 2007) and suggested dust aerosol may be from fly ash and anthropogenic construction. Comparing Fig.4(a) with Fig.4(b), we find although WASO mass proportion is less than DUST, it

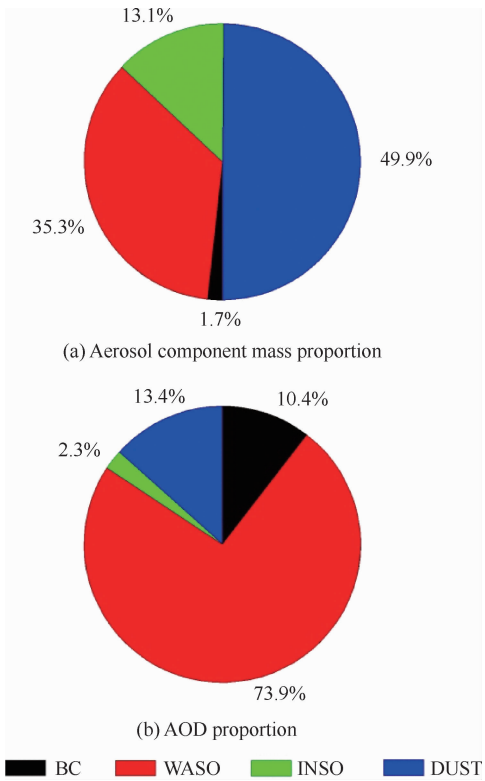

Fig.4 Aerosol component mass proportion and AOD proportion during Jan 2013 in Beijing

contributes to AOD (73.8%)greater than DUST (13.4%). While BC contributes the least to mass proportion (1.7%), the contribution to AOD is 10.4%. As shown in Fig.4(a) and Fig.4(b), anthropogenic aerosol mass proportion is less than natural aerosol (37%), and they contributes to most of the atmosphere extinction (84%).

The contribution of different aerosol components to AOD was shown in Fig.5, and the curve represented relative humidity. We found WASO dominates in total AOD (as shows also in Fig.4(b)). In heave haze days AOD increases rapidly from 0.2 (January 8) to 1.69 (January 11). BC aerosol AOD increases also in certain extent,which may be explained by lower wind speed is lower in haze days blocking black carbon diffusion.

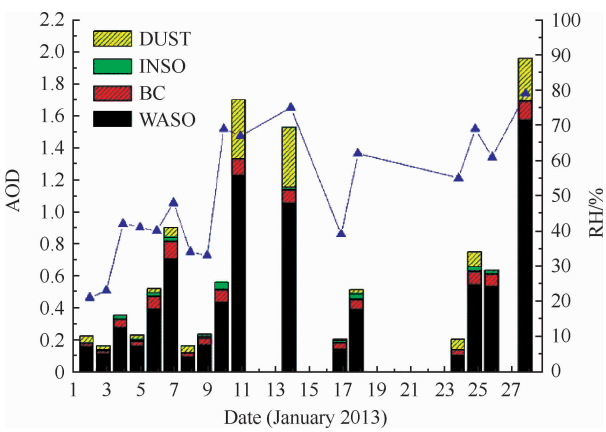

Fig.5 Aerosol components contributes to AOD in Jan. 2013 in Beijing

In severalhaze days, relative humidity is high and wind

speed is less than 2m/s (Li, et al., 2013) which resulted in hard diffusion of SO_2, NO_2 and accelerated hygroscopic of sulfate, nitrate aerosols (Gysel, et al., 2004). In the first haze process (January 5 to 7), WASO increased from 0.16 to 0.7, while in the most serious haze process (January 10 to 14), WASO increased from 0.43 to 1.24. In another heavy haze day (January 28) AOD reached to 1.96 while WASO reached 1.58 and contributing 79% to total AOD.

3.3 Aerosol radiative forcing

In order to illustrate the relationship between aerosol forcing andpollution levels, we selected January 3 (AQI = 50), January 14 (AQI=331) and January 28 (AQI=396) to present in Fig.6.

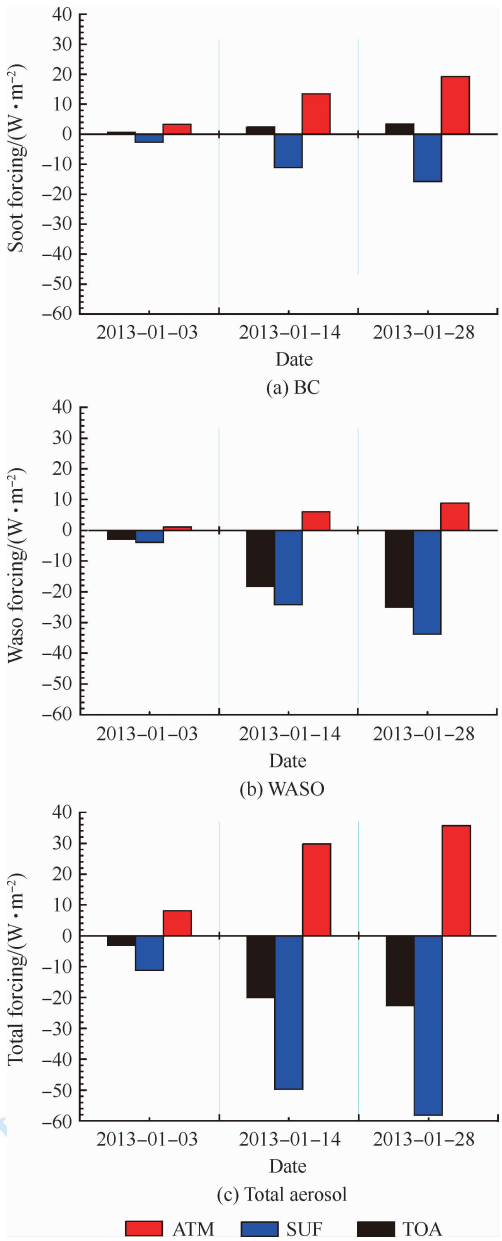

Fig.6 Aerosol forcing in different days

We found aerosol forcing increases while pollution accumulates, and ATM forcing for BC increases significantly, while WASO influences significantly on SUF and TOA forcing. ATM forcing for is 3.3 $W \cdot m^{-2}$ in clean day (January 3), black carbon AOD (AOD_{BC} = 0.02), 13.5 $W \cdot m^{-2}$ and 19.2 $W \cdot m^{-2}$ in heavy polluted days (January 14, AOD_{BC} = 0.09; January 28, AOD_{BC} = 0.12) respectively. Compared AOD of BC with forcing, shows a good relationship between AOD and forcing. Although BC contributed least to AOD and total mass (Fig.4), the percentage contribution of BC to atmosphere forcing is about 50%, suggesting BC aerosol contributes significantly to warming atmosphere.

Atmospheric TOA and SUF forcing can be positive or negative depending on aerosoltypes. For absorbing aerosols (BC) TOA forcing is positive, and SUF forcing is about four times larger than TOA forcing. In the case of scattering aerosols (WASO), its TOA forcing is negative, meanwhile has the same effect and similar magnitude with SUF forcing.

4 CONCLUSION

Ground-based remote sensing measurements and aerosol model have been used to analyze aerosol optical properties, and estimates aerosol direct forcing. The major conclusions include:

(1) Water-soluble aerosol is the major contribution to atmosphere extinction. The contribution of water-soluble aerosol to AOD is about 73%. Besides, while black carbon aerosol contributes less than 2% to the total aerosol mass, it results in a contribution of 10% to AOD.

(2) The relative humidity in heavy haze days is more than 70%, which accelerates the tendency of hygroscopic growth. AOD of water-soluble aerosol increases from 0.15 (January 24) to 1.57 (January 28), which is about 10 times of clean day. Black carbon aerosol shows also the tendency of growth with humidity which increases from 0.015 (January 24) to 0.124 (January 28) which is about eight times of clean day.

(3) Aerosol direct forcing of black carbon and water-soluble aerosols increase in haze days, and show a good correlation with AOD. However, different aerosol types have different influence on forcing. Black carbon contributes most to atmosphere forcing (50%), while water-soluble aerosol contributes more to surface forcing (60%).

Acknowledgements: Authors thank for China Meteorological Administration public service for providing meteorological data.

REFERENCES

Babu S S, Satheesh S K and Moorthy K K. 2002. Aerosol radiative forcing due to enhanced black carbon at an urban site in India. Geophysical Research Letters, 29(18): 1880 [DOI: 10.1029/2002GL015826]

Bond T C and Bergstrom R W. 2006. Light absorption by carbonaceous particles: An investigative review. Aerosol Science and Technology, 40(1): 27-67 [DOI: 10.1080/02786820500421521]

Duan F K, Liu X D, He K B, Li Y W and Dong S P. 2007. Characteristics and source identification of particulate matter in wintertime in Beijing. Water, Air, and Soil Pollution, 180(1-4): 171-183 [DOI: 10.1007/s11270-006-9261-4]

Gysel M, Weingartner E, Nyeki S, Paulsen D, Baltensperger U, Galambos I and Kiss G. 2004. Hygroscopic properties of water-

soluble matter and humic-like organics in atmospheric fine aerosol. Atmospheric Chemistry and Physics, 4(1): 35-50 [DOI: 10.5194/acp-4-35-2004]

Hansen A D A, Rosen H and Novakov T. 1984. The aethalometer—an instrument for the real-time measurement of optical absorption by aerosol particles. Science of the Total Environment, 36: 191-196 [DOI: 10.1016/0048-9697(84)90265-1]

Haywood J M, Roberts D L, Slingo A, Edwards J M and Shine K P. 1997. General circulation model calculations of the direct radiative forcing by anthropogenic sulfate and fossil-fuel soot aerosol. Journal of Climate, 10(7): 1562-1577 [DOI: 10.1175/1520-0442(1997)010<1562:GCMCOT>2.0.CO;2]

Heald C L, Jacob D J, Park R J, Alexander B, Fairlie T D, Yantosca R M and Chu D A. 2006. Transpacific transport of Asian anthropogenic aerosols and its impact on surface air quality in the United States. Journal of Geophysical Research, 111(D14): D14310 [DOI: 10.1029/2005JD006847]

Hess M, Koepke P and Schult I. 1998. Optical properties of aerosols and clouds: The software package OPAC. Bulletin of the American Meteorological Society, 79(5): 831-844 [DOI: 10.1175/1520-0477(1998)079<0831:OPOAAC>2.0.CO;2]

Jiang X Y, Zhang C L, Gao H,Miao S G. 2007. Impacts of urban albedo change on urban heat island in Beijing—a case study. Acta Meteorologica Sinica, 65(2): 301-307

Kaufman Y J, Boucher O, Tanré D, Chin M, Remer L A and Takemura T. 2005a. Aerosol anthropogenic component estimated from satellite data. Geophysical Research Letters, 32(17): L17804 [DOI: 10.1029/2005GL023125]

Kaufman Y J, Koren I, Remer L A, Rosenfeld D and Rudich Y. 2005b. The effect of smoke, dust, and pollution aerosol on shallow cloud development over the Atlantic Ocean. Proceedings of the National Academy of Sciences of the United States of America, 102(32): 11207-11212 [DOI: 10.1073/pnas.0505191102]

Li Z Q, Xu H, Zhang Y, Zhang Y H, Cheng C, Li D H, Li L, Hou W Z, Lv Y, Gu X F. 2013. Joint use of active and passive remote sensing for monitoring of severe haze pollution in Beijing 2013. Journal of Remote Sensing, 17(4): 919-928 [DOI:10.11834/jrs.20133066]

Liu H N, Zhang L. 2002. The climate effects of anthropogenic aerosols of different emission scenarios in China. Chinese Journal of Geophysics, 55(6): 1867-1875

Michalsky J J, Anderson C P, Barnard J, Delamere J, Gueymard C, Kato S, Kiedron P, McComiskey A and Ricchiazzi P. 2006. Shortwave radiative closure studies for clear skies during the atmospheric radiation measurement 2003 aerosol Intensive observation Period. Journal of Geophysical Research, 111(D14) [DOI: 10.1029/2005JD006341]

Penner J E, Chuang C C and Grant K. 1998. Climate forcing by carbonaceous and sulfate aerosols. Climate Dynamics, 14(12): 839-851 [DOI: 10.1007/s003820050259]

Pilinis C, Pandis S N and Seinfeld J H. 1995. Sensitivity of direct climate forcing by atmospheric aerosols to aerosol size and composition. Journal of Geophysical Research, 100(D9): 18739-18754 [DOI: 10.1029/95JD02119]

Ramanathan V, Crutzen P J, Kiehl J T and Rosenfeld D. 2001. Aerosols, climate, and the hydrological cycle. Science, 294(5549): 2119-2124 [DOI: 10.1126/science.1064034]

Ricchiazzi P, Yang S, Gautier C and Sowle D. 1998. SBDART: A research and teaching software tool for plane-parallel radiative transfer in the Earth's atmosphere. Bulletin of the American Meteorological Society, 79(10): 2101-2114 [DOI: 10.1175/1520-0477(1998)079<2101:SARATS>2.0.CO;2]

Satheesh S K and Ramanathan V. 2000. Large differences in tropical aerosol forcing at the top of the atmosphere and Earth's surface. Nature, 405(6782): 60-63 [DOI: 10.1038/35011039]

Shi X H, Xu X D. 2012. Progress in the study of regional impact of aerosol and related features of heavy fog in Beijing City.Chinese Journal of Geophysics, 55(10):3230-3239

Tripathi S N, Dey S, Tare V and Satheesh S K. 2005. Aerosol black carbon radiative forcing at an industrial city in northern India. Geophysical Research Letters, 32(8): L08802 [DOI: 10.1029/2005GL022515]

Wang L, Li Z Q, Tian Q J, Ma Y, Zhang F X, Zhang Y, Li D H, Li K T, Li L. 2012. Retrieval of Dust Fraction of Atmospheric Aerosols Based on Spectra Characteristics of Refractive indices obtained from remote sensing measurements. Spectroscopy and spectral analysis, 32(6): 1644-1649

Wang X H, Shi G Y, Ma X Y.2002. The Direct Radiative Forcing of Anthropogenic Sulfate and Its Temperature Response over the Eastern Asia.Chinese Journal of Atmospheric Sciences, 26(6):751-760

Xie Y S, Li D H, Li K T, Zhang L, Chen C, Xu H and Li Z Q. 2013. Aerosol optical and microphysical properties in haze days based on ground-based remote sensing measurements. Journal of Remote Sensing, 17(4): 970-980 [DOI:10.11834/jrs.20133060]

Yu H B, Dickinson R E, Chin M, Kaufman Y J, Zhou M, Zhou L, Tian Y, Dubovik O and Holben B N. 2004. Direct radiative effect of aerosols as determined from a combination of MODIS retrievals and GOCART simulations. Journal of Geophysical Research, 109(D3): D03206 [DOI: 10.1029/2003JD003914]

Zhang L S, Shi G Y. 2012. The Simulation and Estimation of Radiative Properties and Radiative Forcing due to Sulfate and Soot Aerosols. Chinese Journal of Atmospheric Sciences, 25(2):231-242

灰霾污染状况下气溶胶组分及辐射效应的遥感估算

魏鹏[1,2]，李正强[1]，王堰[1]，谢一淞[1,2]，张莹[1,2]，许华[1]

1.中国科学院遥感与数字地球研究所 国家环境保护卫星遥感重点实验室，北京 100101;

2.中国科学院大学，北京 100049

摘　要:利用地基遥感观测数据和气溶胶模型,分析了北京地区 2013 年 1 月份灰霾期间气溶胶中不同成分的光学特性,并使用大气辐射传输模式估算了气溶胶中不同成分对直接辐射强迫的贡献。结果显示,在严重灰霾时期,大气中的硫酸盐等水溶性气溶胶光学厚度 AOD(440 nm)显著增加,对气溶胶光学厚度的贡献达到 70% 以上,同时黑碳气溶胶对总光学厚度(440 nm)的贡献也呈现增长趋势,是晴朗天气下的 8 倍以上。严重灰霾(2013-01-28)时气溶胶的直接辐射强迫显著增加,但气溶胶中不同成分对辐射强迫的贡献不同,黑碳成分在气溶胶对大气层的辐射强迫中占主要贡献的 57%,而水溶性成分则在气溶胶对地表的辐射强迫中占主要贡献的 60%。

关键词:人为气溶胶,气溶胶模型,辐射效应,地基遥感

中图分类号:X87　　**文献标志码**:A

引用格式:魏鹏,李正强,王堰,谢一淞,张莹,许华. 2013. 灰霾污染状况下气溶胶组分及辐射效应的遥感估算. 遥感学报,17(4):1021-1031

Wei P, Li Z Q, Wang Y, Xie Y S, Zhang Y and Xu Hua. 2013. Remote sensing estimation of aerosol composition and radiative effects in haze days. Journal of Remote Sensing, 17(4): 1021-1031 [DOI: 10.11834/jrs.20133080]

1　引　言

大气气溶胶在影响地球能量收支中起重要作用,主要体现为气溶胶散射和吸收短波辐射而产生的直接效应,以及气溶胶粒子成为云凝结核从而改变云的微物理特性和辐射特性产生的间接效应,并进一步影响全球能量与水循环(Ramanathan 等,2001;Kaufman 等,2005a)。根据大气中气溶胶来源的不同,可以将气溶胶分为自然气溶胶和人为气溶胶。自然气溶胶主要包括火山灰、海盐、沙尘气溶胶等。人为气溶胶主要指人为活动产生的气溶胶,包括矿物燃烧过程中产生的黑碳气溶胶,汽车尾气、工业排放产生的硫酸盐、硝酸盐等水溶性气溶胶。不同类型的气溶胶由于其散射和吸收特性不同,具有不同的辐射效应,例如,硫酸盐气溶胶散射特性较强,所产生的直接辐射强迫一般为负值,而黑碳气溶胶由于其较强的吸收特性,产生的直接辐射强迫为正值,并随时空变化很大(Penner 等,1998)。关于气溶胶的辐射特性及其气候效应已有许多研究成果(Pilinis 等,1995;Satheesh 等,2000),但是目前对于气溶胶中人为成分,如黑碳气溶胶、硫酸盐气溶胶的估计仍然具有很大的不确定性。在估计人为气溶胶辐射效应方面,通常采用模式模拟(Haywood 等,1997;Yu 等,2004;Heald 等,2006),卫星遥感(Kaufman 等,2005b),以及利用区域气候模式(王喜红 等,2002;刘红年和张力,2012)和化学传输模式(张立盛和石广玉,2012)等估算方法。本文利用地基遥感观测数据和气溶胶模型,分析了北京地区 2013 年 1 月份灰霾天气下气溶胶中不同成分特性的变化情况,并使用辐射传输模式估算了气溶胶的直接辐射强迫。

2　数据与方法

2.1　数据

本文采用的观测仪器是位于中国科学院遥感

收稿日期:2013-04-07;**修订日期**:2013-05-31;**优先数字出版日期**:2013-06-07

基金项目:国家重大科学研究计划(编号:2010CB950800);中国科学院战略性先导科技专项(编号:XDA05100202)

第一作者简介:魏鹏(1989—　),男,硕士研究生,现从事大气遥感研究。E-mail:wp5621679@163.com

通信作者简介:李正强(1977—　),男,研究员,现从事大气气溶胶及其辐射效应研究。E-mail: lizq@irsa.ac.cn

与数字地球研究所(奥运村运园区)楼顶的 CE-318 型太阳-天空光度计和 AE-51 型手持黑碳仪。使用数据包括:(1)太阳-天空光度计观测的气溶胶光学厚度(AOD)(440 nm,500 nm,675 nm,870 nm,1020 nm),以及反演得到的单次散射反照率 SSA、不对称因子 g(440 nm,675 nm,870 nm,1020 nm)(谢一淞 等,2013)和水汽柱浓度;(2)黑碳仪观测的近地面黑碳气溶胶质量浓度(Hansen 等,1984);(3)空气相对湿度 RH(中国气象局)。表 1 给出了观测数据基本情况。

表 1　观测数据

数据来源	观测参数	观测时间	有效观测天数/d
CE-318	AOD、SSA、g、水汽柱浓度	2013-01-01—2013-01-28	17
AE-51	黑碳气溶质量浓度	2013-01-01—2013-01-28	12
中国气象局	RH	2013-01-01—2013-01-28	28

2.2　气溶胶模型

为了估算气溶胶不同成分的光学性质,本文采用云与气溶胶光学特性模型 OPAC(Optical Properties of Aerosol and Clouds)进行模拟和分析。OPAC 是 Hess 等人(1998)开发用于计算不同波段(0.3—40 μm)和不同湿度条件下整层大气中气溶胶和云的光学与微物理特性的模型。在 OPAC 模型中气溶胶组分包括水溶性气溶胶(主要为硫酸盐、硝酸盐等)、沙尘气溶胶、黑碳气溶胶、不可溶气溶胶(主要是不可溶有机物)以及海盐气溶胶。OPAC 模型给出了这些不同成分气溶胶在短波波段下(0.35—4.0 μm)的光学与微物理特性,包括光学厚度、消光系数、散射系数、单次散射反照率以及不对称因子。根据北京地区的气溶胶成分研究(王玲等,2012;施晓晖和徐祥德,2012;Wang 等,2013),本文选取 4 种典型成分作为北京地区气溶胶的组成类型,即主要为人为来源的黑碳气溶胶(BC)和水溶性气溶胶(WASO),以及主要为自然来源的沙尘气溶胶(DUST)和不可溶气溶胶(INSO)。

大气中的气溶胶根据其混合方式分为外混合和内混合两种(Bond 和 Bergstrom,2006),在 OPAC 模型中采用的是外混合的方式,即将每种类型的气溶胶的光学性质通过线性相加,计算出混合状态下的整体光学性质和微物理性质(Hess 等,1998)。AOD,SSA 和 g,可以通过不同成分的外混合计算式(1)—式(3)获得(Hess 等,1998):

$$\mathrm{AOD}_\lambda = \sum_i \int \pi r^2 b_{i,\lambda}^{\mathrm{ext}} n_i(r)\,\mathrm{d}r \tag{1}$$

$$\mathrm{SSA}_\lambda = \frac{\sum_i b_{i,\lambda}^{\mathrm{ext}} \mathrm{SSA}_{i,\lambda}}{\sum_i b_{i,\lambda}^{\mathrm{ext}}} \tag{2}$$

$$g_\lambda = \frac{\sum_i b_{i,\lambda}^{\mathrm{sca}} g_{i,\lambda}}{\sum_i b_{i,\lambda}^{\mathrm{sca}}} \tag{3}$$

式中,λ 代表观测波段,i 代表不同成分,r 为气溶胶粒子半径,$n_i(r)$ 代表不同成分的数浓度谱分布,$b_{i,\lambda}^{\mathrm{ext}}$、$b_{i,\lambda}^{\mathrm{sca}}$、$g_{i,\lambda}$ 代表每种成分的消光系数、散射系数和不对称因子。在 OPAC 模型中,单一组分气溶胶的消光系数、散射系数与粒子数浓度存在线性关系(Hess 等,1998),因此可以通过改变不同组分数浓度以获得气溶胶的消光系数。将 AOD、SSA、g 和 RH 的日平均值作为输入参数,迭代条件为:(1)AOD 观测值与模拟值误差小于 0.05;(2)SSA、g 反演值与模拟值误差小于 0.05,最终得到最优解,即每种成分的数浓度。另外,在计算之前,需要考虑参数之间的波段匹配关系,由于模型中对应的光学参数位于 450 nm,500 nm,650 nm,900 nm,1000 nm 波段,因此需要将仪器观测值通过三次拟合内插到模型对应波段上,计算相应的光学参数。该方法流程图如图 1 所示。

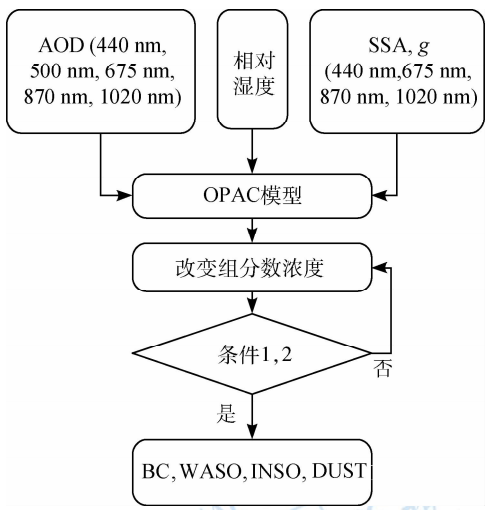

图 1　气溶胶成分反演流程图

本文分别选取了 1 月 2 日清洁天气(AQI = 39,北京市环境监测中心)和 1 月 11 日重度污染天气(AQI = 386)下,观测值与模拟值的拟合结果,如图 2 所示。从图 2 中可以看到不同天气下气溶胶光学厚度具有较好的拟合结果,与观测值的偏差在误差范围以内(0.05)。

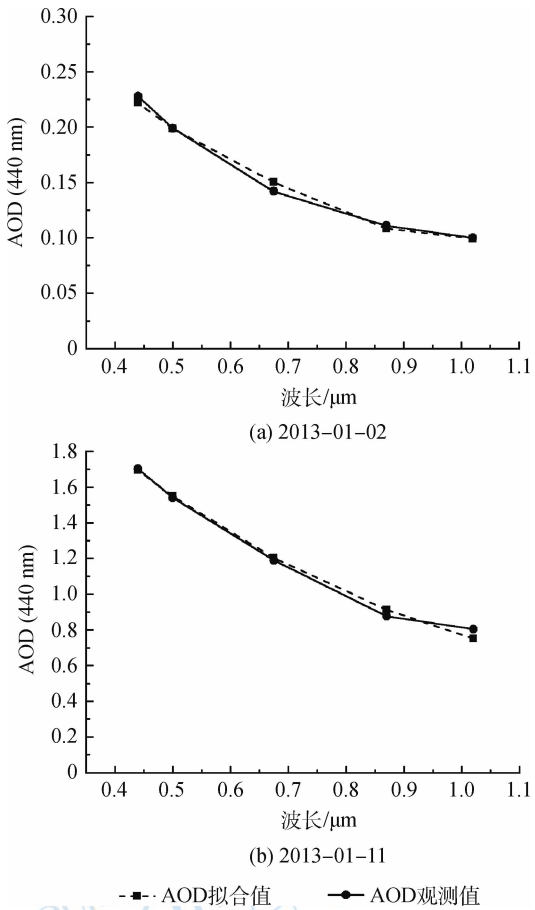

图 2 OPAC 模拟拟合结果

2.3 辐射传输模式

辐射传输模式 SBDART(Santa Barbara DISORT Atmospheric Radiative Transfer)是 Ricchiazzi 等人(1998)用于计算短波波段(0.25—4.0 μm)下地球大气和地球表面平面平行大气的辐射传输模式,广泛应用于计算气溶胶辐射强迫(Babu 等,2002;Tripathi 等,2005)。利用 SBDART 计算的辐射通量和辐射通量观测值的误差范围在±2%以内(Michalsky 等,2006)。在 SBDART 中定义了 6 种标准大气廓线:热带、中纬度夏季、中纬度冬季、副极地夏季、副极地冬季。本文选取的是中纬度冬季标准大气廓线将北京市冬季的地表反射率 0.15(江晓燕 等,2007)作为输入参数。在气溶胶类型的选择上,SBDART 允许自定义气溶胶类型,即通过输入气溶胶光学厚度、单次散射反照率和不对称因子来确定气溶胶类型。本文将 2.2 节中气溶胶模型计算出的气溶胶不同成分的光学参数作为输入,分别计算了有气溶胶状态下的大气层顶(TOA)和地表(SUF)的辐射通量($FLUX_{aerosol}$),以及无气溶胶状态下的大气层顶和地表的辐射通量($FLUX_{no}$),根据式(4)(5)可以计算得到大气层顶与地表的直接辐射强迫(DRF)。

$$DRF_{TOA} = FLUX(TOA)_{aerosol} - FLUX(TOA)_{no} \quad (4)$$

$$DRF_{SUF} = FLUX(SUF)_{aerosol} - FLUX(SUF)_{no} \quad (5)$$

式中,DRF_{TOA} 代表大气层顶的辐射强迫,DRF_{SUF} 代表地表的辐射强迫,$FLUX(TOA)_{aerosol}$ 代表有气溶胶状态下大气层顶的辐射通量,$FLUX(SUF)_{aerosol}$ 代表有气溶胶状态下的地表辐射通量,$FLUX(TOA)_{no}$ 代表无气溶胶状态下的大气层顶的辐射通量,$FLUX(SUF)_{no}$ 代表无气溶胶状态下的地表辐射通量。

大气层(ATM)气溶胶的直接辐射强迫定义为大气层顶的辐射强迫(DRF_{TOA})减去地表的辐射强迫 DRF_{TOA},即

$$DRF_{ATM} = DRF_{TOA} - DRF_{SUF} \quad (6)$$

根据式(6),可以计算得到气溶胶的直接辐射强迫。

3 结果与分析

利用第 2 节中介绍的气溶胶模型分别计算了气溶胶不同成分的光学性质,并与实测结果进行对比,并在辐射传输模式中估算了不同成分的直接辐射强迫。

3.1 黑碳浓度估算及验证

为验证反演结果,本文对比了 1 月份的反演结果和黑碳质量浓度的日平均观测值,有效观测日期为 12 天。根据 OPAC 模型中气溶胶数浓度与质量浓度之间的对应关系,将反演出的黑碳数浓度转化质量浓度,并与日平均观测值进行对比,如图 3 所示,可以看出反演的黑碳质量浓度在总体上与观测值具有较好的相关性,其中相关系数 $R^2 = 0.66$,相对误差为 32%。

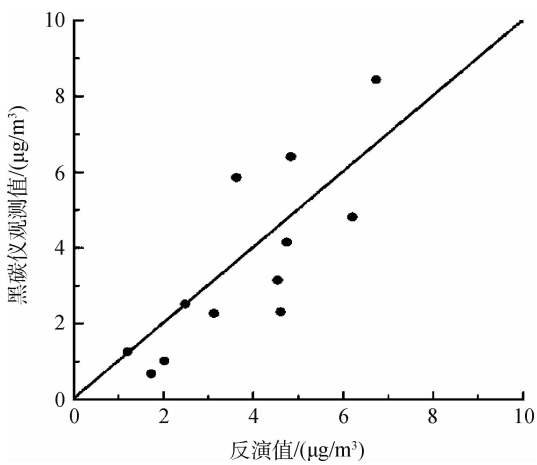

图 3 反演值与黑碳仪观测值的对比

3.2 气溶胶化学组成及光学特性估算

本文利用 OPAC 模型计算了北京地区 2013 年 1 月份气溶胶不同成分的质量比例和光学厚度(440 nm)比例的月平均值，如图 4(a)(b)所示。

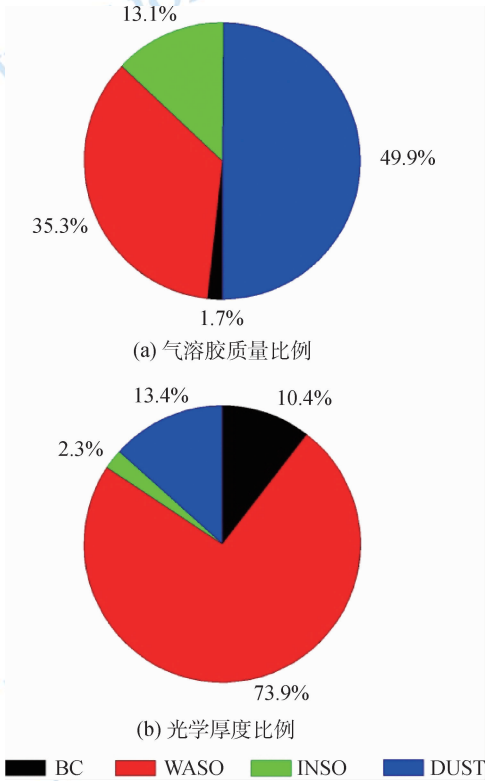

图 4 北京 2013 年 1 月份不同成分的气溶胶质量比例和光学厚度比例

从图 4(a)中可以看到北京地区 1 月份的气溶胶中含量较高的成分是沙尘(49.8%)和水溶性成分(35.3%)。一些地基观测也显示北京冬季近地表的沙尘气溶胶含量较高(Duan 等，2007)，这些沙尘可能与地面扬尘以及施工建设等人为活动有关。对比图 4(a)与图 4(b)可以看到，虽然水溶性气溶胶的质量比例低于沙尘，但在光学厚度比例中却远超过沙尘达 73.8%。含量最少的黑碳气溶胶的占总气溶胶的质量比例为 1.7%，但对光学厚度的贡献达到 10.4%。从图 4(b)中可以看出，人为活动产生的黑碳气溶胶和水溶性气溶胶虽然含量较低(约为 37%)，但是对大气的消光作用却占主要地位，达到了 84%。

图 5 为气溶胶各成分光学厚度(440 nm)月变化，图中曲线代表相对湿度日均值。可以看到，气溶胶光学厚度中水溶性气溶胶占主要成分(从图 4(b)也可看出)。在灰霾严重时期，气溶胶光学厚度有显著增长，从 1 月 8 日的 0.2 增加到 11 日的 1.69。其中，沙尘气溶胶的光学厚度有明显增加，同时，黑碳气溶胶光学厚度也有一定程度的增加(从 0.015 增加到 0.124)，这是因为灰霾天气中风速较低，不利于黑碳气溶胶的扩散。

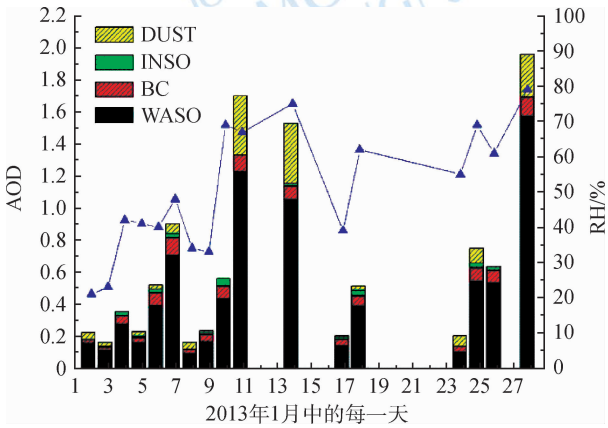

图 5 气溶胶不同成分对总光学厚度贡献月变化

在 2013 年 1 月几次灰霾天气下，相对湿度普遍较高，风速低于 2 m/s(李正强 等，2013)，SO_2、NO_2 气体不易扩散，转化为硫酸盐、硝酸盐等水溶性气溶胶(Gysel 等，2004)，并呈现出吸湿增长特性。在第 1 次灰霾天气期间(1 月 5 日—1 月 7 日)水溶性气溶胶光学厚度从 0.16 增加到 0.7，在最严重的第 2 次灰霾天气中(1 月 10 日—1 月 14 日)水溶性气溶胶光学厚度从 0.43 增加到 1.24。在 28 日另一次严重的灰霾天气中气溶胶光学厚度达到了最大值 1.96，水溶性气溶胶光学厚度也达到了最大值 1.58，占总气溶胶光学厚度的 79%。

3.3 气溶胶辐射强迫估算

为说明气溶胶不同成分的辐射强迫与天气污染程度的关系，本文分别选择了 1 月 3 日(Air Quality Index(AQI)=50)、1 月 14 日(AQI=331)和 1 月 28 日(AQI=396)3 种不同天气下的辐射强迫计算结果作对比分析，如图 6 所示。

可以看出，随着灰霾的加重，气溶胶直接辐射强迫呈现增加趋势，其中，黑碳气溶胶的大气层辐射强迫变化明显(图 6(a))，而水溶性硫酸盐气溶胶对地面辐射强迫和大气层顶辐射强迫影响更大(图 6(b))。黑碳气溶胶对大气层的辐射强迫在良好天气(2013-01-03)为 3.3 $W \cdot m^{-2}$(黑碳气溶胶光学厚度 $AOD_{BC}=0.02$)，重污染天气(2013-01-14)为 13.5 $W \cdot m^{-2}$($AOD_{BC}=0.09$)，重污染天气(2013-01-28)

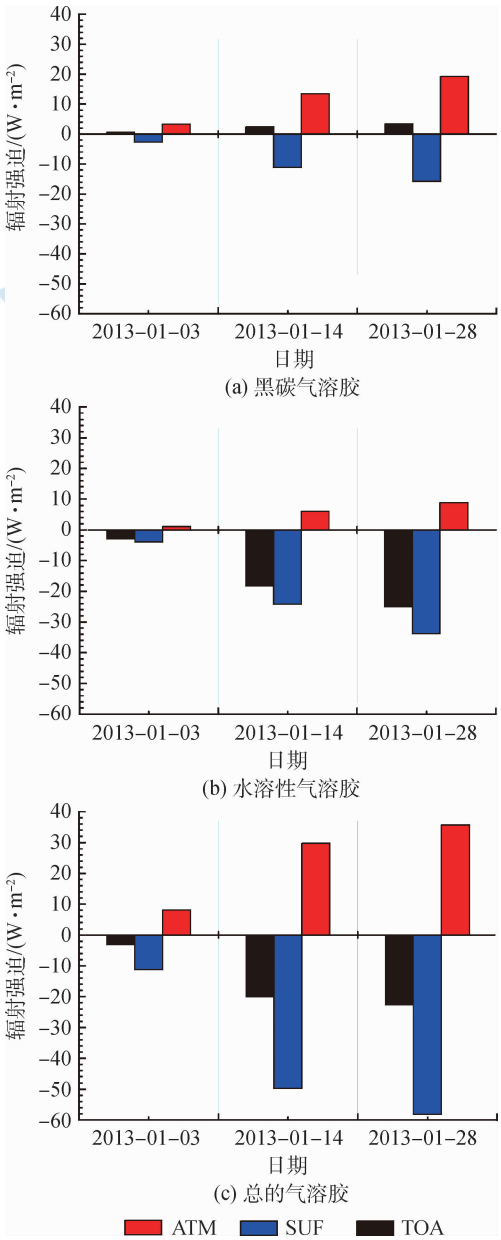

图 6 不同天气下的短波直接辐射强迫

为 19.2 W·m^{-2}(AOD_{BC} = 0.12)。黑碳气溶胶光学厚度在重污染天气分别是良好天气的 4.5 和 6 倍,其大气层的辐射强迫和地面的辐射强迫分别为良好天气的 4.1 和 5.8 倍,说明黑碳气溶胶对大气层的辐射强迫效应与其光学厚度具有较好的一致性。对比图 5 中黑碳气溶胶在总光学厚度的比例,可以看到,黑碳气溶胶虽然含量很低,但是在大气辐射强迫效应中起到了重要作用(>50%)。

此外,对比黑碳气溶胶和水溶性气溶胶,可以看到,两种类型气溶胶对地表都有致冷效应,但是由于水溶性气溶胶的强散射特性,其地表辐射强迫与大气层顶辐射强迫较为接近,而黑碳气溶胶对大气层顶的效应为正效应,并且地表辐射强迫与大气层顶辐射强迫差异较大,是大气层顶辐射强迫的 4 倍。

4 结 论

本文利用 2013 年 1 月份的地基遥感观测数据和气溶胶模型,分析了不同类型气溶胶的光学特性,并结合辐射传输模式估算了辐射强迫。结果显示:

(1)在本次灰霾天气中,气溶胶成分对大气消光的贡献主要来自于水溶性气溶胶成分,其光学厚度比例达到了 73%。此外,虽然黑碳成分在气溶胶中含量低于 2%,但是对光学厚度的贡献超过 10%。

(2)严重雾霾天气中,湿度超过 70% 时,水溶性气溶胶成分呈现增长的趋势,其 AOD 从 0.15(2013-01-24)增加到 1.57(2013-01-28),是清洁天气下的 10 倍。黑碳气溶胶也呈现增长的趋势 ,从 0.015(2013-01-24)增加到 0.124(2013-01-28),增加了 8 倍左右。

(3)气溶胶直接辐射强迫方面,黑碳气溶胶和水溶性气溶胶成分在灰霾时都明显增加,两者的辐射效应与光学厚度之间具有较好的相关性。但不同类型气溶胶对大气的辐射效应不同,在对大气层辐射强迫方面,更多的来自于黑碳气溶胶,占总气溶胶大气层辐射强迫的约 50%,而在地表辐射强迫方面,则更多来自水溶性气溶胶,占总气溶胶地表辐射强迫的 60%。

志 谢 感谢中国气象局公共气象服务中心提供的气象资料。

参考文献(References)

Babu S S, Satheesh S K and Moorthy K K. 2002. Aerosol radiative forcing due to enhanced black carbon at an urban site in India. Geophysical Research Letters, 29(18): 1880 [DOI: 10.1029/2002GL015826]

Bond T C and Bergstrom R W. 2006. Light absorption by carbonaceous particles: An investigative review. Aerosol Science and Technology, 40(1): 27-67 [DOI: 10.1080/02786820500421521]

Duan F K, Liu X D, He K B, Li Y W and Dong S P. 2007. Characteristics and source identification of particulate matter in wintertime in Beijing. Water, Air, and Soil Pollution, 180(1-4): 171-183 [DOI: 10.1007/s11270-006-9261-4]

Gysel M, Weingartner E, Nyeki S, Paulsen D, Baltensperger U, Galambos I and Kiss G. 2004. Hygroscopic properties of water-soluble matter and humic-like organics in atmospheric fine aerosol. Atmospheric Chemistry and Physics, 4(1): 35-50 [DOI: 10.5194/

acp-4-35-2004]

Hansen A D A, Rosen H and Novakov T. 1984. The aethalometer—an instrument for the real-time measurement of optical absorption by aerosol particles. Science of the Total Environment, 36: 191-196 [DOI: 10.1016/0048-9697(84)90265-1]

Haywood J M, Roberts D L, Slingo A, Edwards J M and Shine K P. 1997. General circulation model calculations of the direct radiative forcing by anthropogenic sulfate and fossil-fuel soot aerosol. Journal of Climate, 10(7): 1562-1577 [DOI: 10.1175/1520-0442(1997)010<1562:GCMCOT>2.0.CO;2]

Heald C L, Jacob D J, Park R J, Alexander B, Fairlie T D, Yantosca R M and Chu D A. 2006. Transpacific transport of Asian anthropogenic aerosols and its impact on surface air quality in the United States. Journal of Geophysical Research, 111(D14): D14310 [DOI: 10.1029/2005JD006847]

Hess M, Koepke P and Schult I. 1998. Optical properties of aerosols and clouds: The software package OPAC. Bulletin of the American Meteorological Society, 79(5): 831-844 [DOI: 10.1175/1520-0477(1998)079<0831:OPOAAC>2.0.CO;2]

江晓燕, 张朝林, 高华, 苗世光. 2007. 城市下垫面反照率变化对北京市热岛过程的影响——个例分析. 气象学报, 65(2): 301-307

Kaufman Y J, Boucher O, Tanré D, Chin M, Remer L A and Takemura T. 2005a. Aerosol anthropogenic component estimated from satellite data. Geophysical Research Letters, 32(17): L17804 [DOI: 10.1029/2005GL023125]

Kaufman Y J, Koren I, Remer L A, Rosenfeld D and Rudich Y. 2005b. The effect of smoke, dust, and pollution aerosol on shallow cloud development over the Atlantic Ocean. Proceedings of the National Academy of Sciences of the United States of America, 102(32): 11207-11212 [DOI: 10.1073/pnas.0505191102]

李正强, 许华, 张莹, 张玉环, 陈澄, 李东辉, 李莉, 侯伟真, 吕阳, 顾行发. 2013. 北京区域2013 严重灰霾污染的主被动遥感监测. 遥感学报, 17(4): 919-928［DOI:10.11834/jrs.20133066］

刘红年, 张力. 2012. 中国不同排放情景下人为气溶胶的气候效应. 地球物理科学, 55(6): 1867-1875

Michalsky J J, Anderson C P, Barnard J, Delamere J, Gueymard C, Kato S, Kiedron P, McComiskey A and Ricchiazzi P. 2006. Shortwave radiative closure studies for clear skies during the atmospheric radiation measurement 2003 aerosol Intensive observation Period. Journal of Geophysical Research, 111(D14)［DOI: 10.1029/2005JD006341］

Penner J E, Chuang C C and Grant K. 1998. Climate forcing by carbonaceous and sulfate aerosols. Climate Dynamics, 14(12): 839-851 [DOI: 10.1007/s003820050259]

Pilinis C, Pandis S N and Seinfeld J H. 1995. Sensitivity of direct climate forcing by atmospheric aerosols to aerosol size and composition. Journal of Geophysical Research, 100(D9): 18739-18754 [DOI: 10.1029/95JD02119]

Ramanathan V, Crutzen P J, Kiehl J T and Rosenfeld D. 2001. Aerosols, climate, and the hydrological cycle. Science, 294(5549): 2119-2124 [DOI: 10.1126/science.1064034]

Ricchiazzi P, Yang S, Gautier C and Sowle D. 1998. SBDART: A research and teaching software tool for plane-parallel radiative transfer in the Earth's atmosphere. Bulletin of the American Meteorological Society, 79(10): 2101-2114 [DOI: 10.1175/1520-0477(1998)079<2101:SARATS>2.0.CO;2]

Satheesh S K and Ramanathan V. 2000. Large differences in tropical aerosol forcing at the top of the atmosphere and Earth's surface. Nature, 405(6782): 60-63 [DOI: 10.1038/35011039]

施晓晖, 徐祥德. 2012. 北京及周边气溶胶区域影响与大雾相关特征的研究进展. 地球物理学报, 55(10): 3230-3239

Tripathi S N, Dey S, Tare V and Satheesh S K. 2005. Aerosol black carbon radiative forcing at an industrial city in northern India. Geophysical Research Letters, 32(8): L08802 [DOI: 10.1029/2005GL022515]

王玲, 李正强, 李东辉, 李凯涛, 田庆久, 李莉, 张莹, 吕阳, 顾行发. 2012. 基于遥感观测的折射指数光谱特性反演大气气溶胶中沙尘组分含量. 光谱学与光谱分析, 32(6): 1644-1649

王喜红, 石广玉, 马晓燕. 2002. 东亚地区对流层人为硫酸盐辐射强迫及其温度响应. 大气科学, 26(6): 751-760

谢一淞, 李东辉, 李凯涛, 张龙, 陈澄, 许华, 李正强. 2013. 基于地基遥感的灰霾气溶胶光学及微物理特性观测研究. 遥感学报, 17(4): 970-980［DOI:10.11834/jrs.20133060］

Yu H B, Dickinson R E, Chin M, Kaufman Y J, Zhou M, Zhou L, Tian Y, Dubovik O and Holben B N. 2004. Direct radiative effect of aerosols as determined from a combination of MODIS retrievals and GOCART simulations. Journal of Geophysical Research, 109(D3): D03206 [DOI: 10.1029/2003JD003914]

张立盛, 石广玉. 2012. 硫酸盐和烟尘气溶胶辐射特性及辐射强迫的模拟估算. 大气科学, 25(2): 231-242

遥感学报

启功先生创刊题名

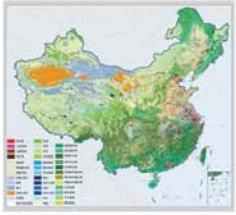

封面说明

About the Cover

2010年中国土地覆被遥感监测数据集（ChinaCover2010）

The China National Land Cover Data for 2010 (ChinaCover2010)

2010年中国土地覆被遥感监测数据集（ChinaCover2010）由中国科学院遥感与数字地球研究所联合其他9个单位历时两年完成，应用30 m空间分辨率的环境星（HJ-1A/1B）数据，利用联合国粮农组织（FAO）的LCCS分类工具，构建了适用于中国生态特征的38类土地覆被分类系统，采用基于超算平台的数据预处理、面向对象的自动分类、地面调查获得的10万个野外样本以及雷达数据辅助分类相结合的方法，数据精度达到85%。ChinaCover2010主要基于国产卫星影像，将遥感与生态紧密结合，充足的野外样点以及严格的产品质量控制在最大程度上保证了数据的精度，可为中国生态环境变化评估以及生态系统碳估算提供基础数据支撑。（网址：http://www.chinacover.org.cn)

The China National Land Cover Data for 2010 (ChinaCover2010) has been completed after two years of team effort by the Institute of Remote Sensing and Digital Earth (RADI), Chinese Academy of Sciences (CAS), together with nine other institutions' participation. The HJ-1A/1B satellite at 30 m resolution is main data source. Based on the landscape features in China, 38 land cover classes have been defined using UN FAO Land Cover Classification System (LCCS). Super computers were used in the data preprocessing. An object-oriented method and a thorough field survey (about 100000 field samples) were used in the land cover classification, with radar imagery as auxiliary data. The overall accuracy of ChinaCover2010 is around 85%. Mainly based on domestic imagery, the products take advantage of various in situ data and strict quality control. ChinaCover2010 is a good dataset for ecological environment change assessment and terrestrial carbon budget studies. (Website: http://www.chinacover.org.cn)

遥感学报

JOURNAL OF REMOTE SENSING

YAOGAN XUEBAO（双月刊　1997年创刊）

第17卷　第4期　2013年7月25日

(Bimonthly, Started in 1997)

Vol.17 No.4 July 25, 2013

主　管	中国科学院	Superintended by	Chinese Academy of Sciences
主　办	中国科学院遥感与数字地球研究所 中国地理学会环境遥感分会	Sponsored by	Institute of Remote Sensing and Digital Earth,CAS The Associate on Environment Remote Sensing of China
主　编	顾行发	Editor-in-Chief	GU Xing-fa
编　辑	《遥感学报》编委会 北京市安外大屯路中国科学院遥感与数字地球研究所 邮编：100101　电话：86-10-64806643 http://www.jors.cn E-mail:jrs@irsa.ac.cn	Edited by	Editorial Board of Journal of Remote Sensing Add: P.O.Box 9718, Beijing 100101, China Tel: 86-10-64806643 http://www.jors.cn E-mail: jrs@irsa.ac.cn
出　版	科学出版社	Published by	Science Press
印刷装订	北京科信印刷有限公司	Printed by	Beijing Kexin Printing Co. Ltd.
总发行	科学出版社 北京东黄城根北街16号 邮政编码：100717 电话：86-10-64017032 E-mail:sales_journal@mail.sciencep.com	Distributed by	Science Press Add: 16 Donghuangchenggen North Street, Beijing 100717, China Tel: 86-10-64017032 E-mail: sales_journal@mail.sciencep.com
国外发行	中国国际图书贸易总公司 北京399信箱　邮政编码：100044	Overseas distributed by	China International Book Trading Corporation Add: P.O.Box 399, Beijing 100044, China

中国标准连续出版物号：ISSN 1007-4619 / CN 11-3841/TP

CODEN YXAUAB

国内邮发代号：82-324

国外发行代号：BM 1002

定价：70.00元

ISSN 1007-4619

9 771007 461132 07

国内外公开发行